Tuomisto, Filip

Vacancy defects in III-nitrides: what does positron annihilation spectroscopy reveal?

Vacancy defects in III-nitrides: what does positron annihilation spectroscopy reveal?

You may also be interested in:

Defect studies with positrons: What could we learn on III-nitride heterostructures?
Filip Tuomisto, Jussi-Matti Mäki, Olli Svensk et al.

Dominant intrinsic acceptors in GaN and ZnO
K Saarinen, S Hautakangas and F Tuomisto

Detection of vacancy-like defects during Cu diffusion in GaAs by positron annihilation
M Elsayed, V Bondarenko, K Petters et al.

Cation vacancies and electrical compensation in Sb-doped thin-film SnO2 and ZnO
E Korhonen, V Prozheeva, F Tuomisto et al.

Properties of optically active vacancy clusters in type IIa diamond
J-M Mäki, F Tuomisto, C J Kelly et al.

Vacancy-donor complexes in highly n-type Ge doped with As, P and Sb
J Kujala, T Südkamp, J Slotte et al.

Determination of defect content and defect profile in semiconductor heterostructures
A Zubiaga, J A Garcia, F Plazaola et al.

Positron annihilation and the charge states of the phosphorus-vacancy pair in silicon
J Makinen, P Hautojarvi and C Corbel

Positron annihilation in neutron irradiated iron-based materials
M Lambrecht and A Almazouzi

Vacancy defects in III-nitrides: what does positron annihilation spectroscopy reveal?

Filip Tuomisto

Department of Applied Physics, Aalto University, P.O. Box 11100, FI-00076 Aalto, Finland

E-mail: filip.tuomisto@tkk.fi

Abstract. The purpose of this paper is to present a short review and comparison of the results obtained with positron annihilation spectroscopy studies of vacancy defects in AlN, GaN and InN. The combination of positron lifetime and Doppler broadening techniques with theoretical calculations has provided the means to deduce both the identities and the concentrations of the vacancies in these materials, while performing measurements as a function of temperature has given information on the charge states of the detected defects. The III-sublattice vacancies are common defects in all the III-nitrides, and they compensate donors either by forming vacancy-impurity complexes or by providing deep states for electrons. In some cases, N vacancies have also been observed.

1. Introduction

The material family of the III-nitrides is a class of important semiconductor materials for applications in optoelectronics at blue and ultraviolet wavelengths and electronic devices operating at high temperatures and high voltage. The importance of intrinsic point defects in nitrides is due to their role in determining the electrical and optical properties of the material, as well as their influence on the material behavior in various processing steps such as ion implantation and thermal annealing. Point defects are created in semiconductor materials during growth, where their formation is governed by thermodynamics and growth kinetics. They can be introduced in concentrations much larger than those given by the thermodynamic equilibrium by means of irradiation of the material, e.g., by electrons. The study of the formation of point defects in different conditions hence yields important information on the basic physical properties of the semiconductor materials in question.

Positron annihilation spectroscopy is an effective method for the investigation of vacancy-type defects in semiconductors. Positrons implanted into a sample can get trapped in and localize at neutral and negative vacancies due to the missing positive ion core. This results in observable changes in the measurable annihilation characteristics, i.e. the positron lifetime and the momentum distribution of the annihilating positron-electron pair (Doppler broadening). The annihilation data can be used to determine the vacancy concentration as well as to distinguish between different vacancy types and their chemical environment.

Positron studies have now been performed in nitride semiconductors for about 10 years after the identification of the Ga vacancy in bulk GaN crystals [1]. In this paper, a short review of the knowledge obtained by positron annihilation spectroscopy on the vacancy defects in nitrides is given, concentrating on the recent results on group-III vacancies and related complexes. The results obtained in GaN, InN and AlN are compared and the similarities and differences are discussed.

2. Experimental details

2.1. Measurements in bulk crystals

The positron lifetimes in bulk crystals were measured with a conventional fast-fast coincidence spectrometer with a time resolution of 250 ps [2]. Two identical sample pieces were sandwiched with a 20 μCi positron source (^{22}Na deposited on 1.5 μm Al foil). Typically 2×10^6 annihilation events were collected in each positron lifetime spectrum. The lifetime spectrum $n(t) = \Sigma_i I_i \exp(-t/\tau_i)$ was analyzed as the sum of exponential decay components convoluted with the Gaussian resolution function of the spectrometer after subtracting the constant background and annihilations in the source material (typically a few percent, for details see *e.g.* Ref. [3]) The positron in state i annihilates with a lifetime τ_i and an intensity I_i. The state in question can be the delocalized state in the lattice or the localized state at a vacancy defect. The increase of the average lifetime $\tau_{\mathrm{ave}} = \Sigma_i I_i \tau_i$ above the bulk lattice lifetime τ_B shows that vacancy defects are present in the material. This parameter that coincides with the center of mass of the spectrum is insensitive to the decomposition procedure, and even a change as small as 1 ps in its value can be reliably measured. In the case of one type of vacancy defect with specific lifetime τ_V, the decomposition of the lifetime spectrum into two components τ_1 and τ_2 is straightforward to interpret. The second lifetime component $\tau_2 = \tau_V$ gives directly the vacancy specific lifetime and the first lifetime component is $\tau_1 = (\tau_B^{-1} + \kappa_V)^{-1} < \tau_B$, where τ_B is the positron lifetime in the delocalized state in the lattice and κ_V the positron trapping rate into the vacancy defects.

The temperature dependence of the average positron lifetime τ_{ave} is analyzed with the model of trapping and escape rates of positrons, explained in detail in earlier works [2, 4, 5, 6]. In this model, the trapping coefficient μ_V to a neutral vacancy is independent of temperature and to a negatively charged vacancy it varies as $T^{-0.5}$. The trapping rate of positrons into the vacancies (concentration c_V) is $\kappa_V = \mu_V c_V$ ($\mu_V = 3 \times 10^{15}$ cm^{3}s^{-1} for Ga vacancies in GaN at 300 K). Positrons can get trapped also at hydrogen-like Rydberg states surrounding negative-ion-type defects (shallow traps for positrons). The positron trapping rate at the Rydberg state μ_R varies also as $T^{-0.5}$, which is the result predicted by theory for the transition from a free state to a bound state in a Coulomb potential [6]. The thermal escape rate from the Rydberg state can be written as

$$\delta_{st} = \mu_R \left(\frac{m_+ k_B T}{2\pi\hbar^2} \right)^{3/2} \exp\left(-\frac{E_{b,st}}{k_B T} \right) \tag{1}$$

where μ_R is the positron trapping coefficient to the lowest hydrogen-like Rydberg state, $E_{b,st}$ is the positron binding energy of the lowest Rydberg state (typically < 0.1 eV), and $m_+ \cong m_0$ is the effective mass of the positron. In principle, positrons can also escape from the Rydberg states around negatively charged vacancies, but we assume that the transition from the Rydberg state to the ground state in the vacancy is fast enough so that this effect can be neglected. An effective trapping rate of the shallow traps can thus be defined as

$$\kappa_{st}^{eff} = \frac{\kappa_{st}}{1 + \delta_{st}/\lambda_{st}} \tag{2}$$

where $\lambda_{st} \cong \lambda_B$ is the annihilation rate of positrons trapped at the Rydberg state, which coincides with the annihilation rate λ_B from the delocalized state in the bulk lattice, and $\kappa_{st} = \mu_R c_{st}$ is directly related to the concentration of the negative ions.

Finally, the decomposition of the lifetime spectra into several lifetime components gives the possibility to determine experimentally the fractions of positrons annihilating in various states. The average lifetime can be written as [2]

$$\tau_{ave} = \eta_B \tau_B + \sum_j \eta_{D,j} \tau_{D,j}, \tag{3}$$

where η_B and τ_B are the annihilation fraction and positron lifetime in the free state in the lattice, and $\eta_{D,j}$ and $\tau_{D,j}$ are the corresponding values in bound states at the defect D_j. The annihilation fractions are related to the trapping rates through

$$\eta_B = \frac{\lambda_B}{\lambda_B + \sum_j \kappa_{D,j}^{eff}}, \quad \eta_{D,j} = \frac{\kappa_{D,j}^{eff}}{\lambda_B + \sum_j \kappa_{D,j}^{eff}}. \tag{4}$$

2.2. Measurements in epitaxial thin films

The positron annihilation characteristics were measured in thin epitaxial films by using a mono-energetic continuous positron beam. As lifetime experiments are not possible with a continuous beam, the Doppler broadening of the annihilation radiation was monitored as a function of the beam energy, providing a depth profile of the signal. The motion of the annihilating electron-positron pair causes a Doppler shift in the annihilation radiation $\Delta E = c p_L / 2$, where p_L is the longitudinal momentum component of the pair in the direction of the annihilation photon emission. This causes the broadening of the 511 keV annihilation line. The shape of the 511 keV peak gives thus the one-dimensional momentum distribution $\rho(p_L)$ of the annihilating electron-positron pairs. A Doppler shift of 1 keV corresponds to a momentum value of $p_L = 0.54$ a.u ($\approx 3.91 \times 10^{-3}\ m_0 c$).

The Doppler broadening can be experimentally measured using a Ge gamma ray detector with a good energy resolution. The typical resolution of a detector is around 1–1.5 keV at 500 keV. This is considerable compared to the total width of 2–3 keV of the annihilation peak meaning that the experimental lineshape is strongly influenced by the detector resolution. Therefore, various shape parameters are used to characterize the 511 keV line. The low electron-momentum parameter S is defined as the ratio of the counts in the central region (typically $p_L < 0.4$ a.u.) of the annihilation line to the total number of the counts in the line. In the same way, the high electron-momentum parameter W is the fraction of the counts in the wing regions of the line (typically $p_L > 1.5$ a.u.). Due to their low momenta, mainly valence electrons contribute to the region of the S parameter. On the other hand, only core electrons have momentum values high enough to contribute to the W parameter. Therefore, S and W are sometimes called the valence and core annihilation parameters, respectively. The S and W parameters are related to the annihilation fractions in a similar manner as the average positron lifetime in Eq. (3).

The high-momentum part of the Doppler broadening spectrum arises from annihilations with core electrons that contain information on the chemical identity of the atoms. Thus the detailed investigation of core electron annihilation can reveal the nature of the atoms in the regions where positrons annihilate. In order to study the high-momentum part in detail, the experimental background needs to be reduced. A second gamma ray detector can be placed opposite to the Ge detector and the only events that are accepted are those for which both 511 keV photons are detected [7, 8]. Depending on the type of the second detector, electron momenta even up to $p \approx 8$ a.u. ($\approx 60 \times 10^{-3}\ m_0 c$) can be measured with the coincidence detection of the Doppler broadening.

3. Vacancy defects in GaN

Since the identification of native Ga vacancies by positron annihilation spectroscopy in high nitrogen pressure (HNP) grown bulk GaN crystals [1], more than a hundred studies of GaN with positrons have been published [9]. In the following, some of the main findings about the nature of vacancy defects in GaN are presented. Figure 1 shows the average positron lifetime measured in a variety of thick bulk or quasi-bulk GaN samples. The average positron lifetime (τ_{ave}) in most of the measured GaN samples is

above the bulk lifetime of 160 ps [10] ($\tau_{ave} > \tau_B$ = 160 ps) in some temperature range, indicating that positrons annihilate as trapped at vacancy defects. These vacancies have been identified as Ga vacancies by the second lifetime component of τ_2 = 235 ± 10 ps (figure 1b) separated from the lifetime spectra [1, 10–12]. The temperature dependence of the average positron lifetime in O-doped and undoped GaN samples grown by hydride vapor phase epitaxy (HVPE) shows enhanced positron trapping at Ga vacancies at low temperatures, indicating that the Ga vacancies are negatively charged. On the other hand, the temperature dependence of τ_{ave} in the GaN samples grown by the high nitrogen pressure (HNP) method indicates that negative non-open volume defects that act as shallow traps for positrons compete in positron trapping with the Ga vacancies at low temperatures. These negative centers have been identified as Mg_{Ga}^- acceptors in the HNP GaN samples by comparing to data obtained with secondary ion mass spectrometry [1, 10]. The lack of these shallow traps in the undoped and O-doped HVPE GaN samples in figure 1 and in the data in Refs. [11–13] implies that Ga vacancies are the dominant intrinsic acceptor defects in *n*-type GaN when impurities acting as acceptors are not present [14]. This conclusion has also been confirmed by the very good match of vacancy and total acceptor densities, obtained by combining positron annihilation and temperature-dependent Hall measurements [13]. The experiments have also shown the universal role of the Ga vacancy as the most important compensating acceptor over four orders of magnitude of intentional oxygen doping [11].

By combining positron lifetime and coincidence Doppler broadening experiments with state-of-the-art theoretical calculations, the in-grown Ga vacancy defects in GaN with sufficient O content have been identified as V_{Ga}–O_N pairs [11, 15]. In contrast, in electron irradiation experiments [12, 16], isolated Ga vacancies are produced. Figure 1 shows also the average positron lifetime measured in an as-irradiated (2-MeV electrons at room temperature) undoped HVPE-GaN sample and a sample subsequently annealed at 775 K. It can be seen from figure 1b that the second lifetime components extracted from the lifetime spectra are the same in the case of in-grown O-complexed and isolated Ga vacancies, in good agreement with theory [11]. The average positron lifetime in the as-irradiated sample shows the coexistence of a high concentration of Ga vacancies and irradiation-induced (and hence intrinsic) negative ions. Interestingly, after the annealing at 775 K, the temperature threshold for positron escape from these negative ions changes indicating a change in the binding energy of positrons to these defects. This has been interpreted as a change in the charge state (from 2^- to 1^-) of the negative ions.

The electron irradiation experiments [12, 16] have shown that the migration barrier of the isolated Ga vacancies is E_M = 1.8 ± 0.2 eV. Annealing experiments in as-grown HVPE GaN samples at high temperatures and high nitrogen pressure, where a redistribution of the V_{Ga}–O_N pairs [15, 17, 18] was observed, have given the possibility to determine the binding energy of the pair as E_B =1.6 ± 0.2 eV. This is in excellent agreement with theoretical results [19, 20]. Also the theoretical prediction about the formation energy of the isolated Ga vacancy was confirmed in those experiments. Studies of the differences in Ga vacancy distributions in GaN grown in the Ga- and N-polar directions as well as in non-polar directions, both in homo- and hetero-epitaxial HVPE samples, have given further information on the formation of the V_{Ga}–O_N pairs [3, 10, 21, 22]. These results demonstrate that Ga vacancies are created thermally as isolated at the high growth temperatures in both HVPE and HNP GaN, but their ability to form V_{Ga}–O_N complexes determines the fraction of vacancy defects surviving the cooling down. In addition, those results show that the O incorporation from the growth ambient and the subsequent vacancy formation depends on the growth polarity due to the different sticking coefficients of O for different growth surfaces. It is important to note that Si doping does not have the same effect, as the binding between the Si donors and Ga vacancies is much less efficient due to the larger distance between the individual acceptor (Ga vacancy) and donor (substitutional Si) defects [23].
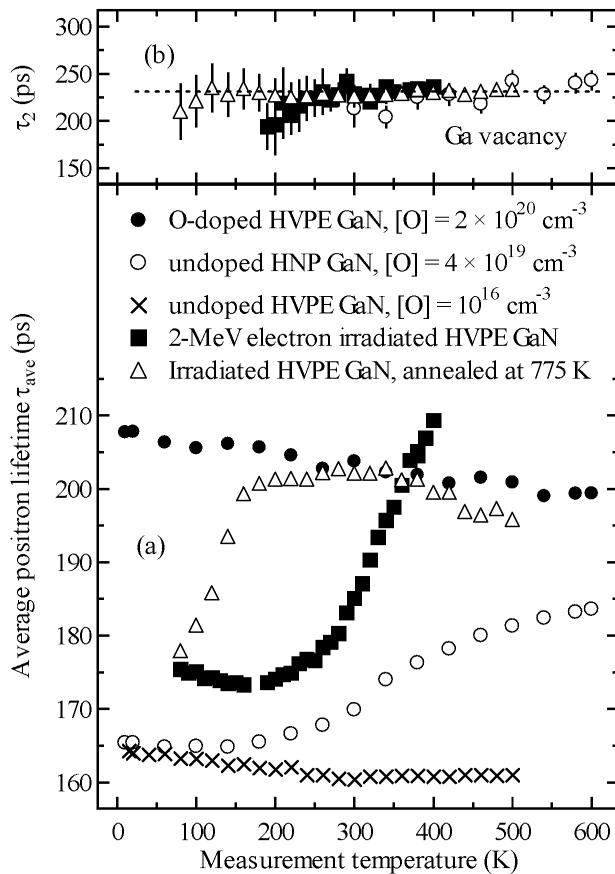
Figure 1. (a) The average positron lifetime measured as a function of temperature in different thick bulk or quasi-bulk GaN samples. Vacancies are present when the average positron lifetime is above the bulk lifetime of $\tau_B \approx 160$ ps. The temperature dependence of the average positron lifetime demonstrates the different effects of negative charge of both the vacancies and acceptor-type impurities. (b) The second lifetime component extracted from the lifetime spectra is the same, $\tau_2 \approx 235$ ps, in all the measured samples. This component is attributed to Ga vacancies, either isolated or complexed with O impurities.

The above presented results show that Ga vacancies act as dominant compensating centers in *n*-type GaN. On the other hand, in *p*-type GaN, where the formation of Ga vacancies is energetically unfavourable due their acceptor nature, the natural question is whether N vacancies could compensate the doping. The detection of vacancy defects on the N sublattice with positrons is not evident due to the small open volume generated by the missing N atom. Nevertheless evidence of the existence of N vacancies complexed with Mg (V_N-Mg_{Ga}) has been obtained with positrons in Mg-doped (*p*-type) GaN grown by metal-organic chemical vapour deposition (MOCVD) [24,25]. It is worth noting that even though the vacancy concentrations are similar relative to the doping densities (a few percent at most) in both *n*- and *p*-type GaN, the vacancies are dominant compensating centers only in *n*-type GaN, while in *p*-type GaN other defects and impurities such as hydrogen play the most important role. Isolated neutral N vacancies have also been provisionally identified in electron-irradiated (0.5 MeV energy) samples recently [12].

The effects of varying growth conditions (such as temperature, stoichiometry and growth polarity) have been studied with a slow positron beam in a variety of thin film samples grown by either molecular beam epitaxy (MBE) [26] or MOCVD [23, 27]. These studies show that the growth stoichiometry has a very strong impact on the formation of Ga vacancies: the more N rich the growth, the more there are Ga vacancies in the material. Also a higher growth temperature results in a higher Ga vacancy concentration. Interestingly, these findings hold also when comparing the thin-film techniques to bulk or quasi-bulk growth techniques, suggesting that the formation of Ga vacancies is governed by thermodynamical effects irrespective of the growth method. This conclusion is supported by the results obtained in samples grown with various polarities [3, 10, 21, 22], where it has been observed that the sticking of O on different growth surfaces and the following differences in O content in the material dictate the formation of Ga vacancies (in addition to the growth stoichiometry).

4. Vacancy defects in InN and AlN

The other two nitrides, *i.e.*, InN and AlN, have been far less studied with positrons than GaN [9]. The reason for this has been the lack of suitable samples of sufficiently high quality, and especially in the case of InN, the inexistence of (thick) bulk samples. However, the material quality has improved significantly over the past couple of years, and extensive studies of InN and AlN with positrons should be anticipated.

4.1. Vacancy defects in InN

Figure 2 shows the S parameter measured at room temperature as a function of positron implantation energy in MBE-grown InN samples of different thicknesses and dates of growth (2002 vs. 2006) [28, 29]. When positrons are implanted close to the sample surface with E = 0 – 1 keV, the same S parameter of S = 0.48 is recorded in all the InN samples. These values characterize the defects and chemical nature of the near-surface region of the samples at the depth 0 – 5 nm. The region of constant S is different from sample to sample due to the different thicknesses of the layers, and extends from a few keV up to 30 keV in the thickest sample. The data recorded at the energies where S is constant can be taken as characteristic of the layer. The decrease of the S parameter at higher implantation energies is due to the increasing fraction of positrons annihilating in the sapphire substrate, for which the characteristic S parameter is roughly S = 0.41. It is clearly seen that the S parameter of InN decreases with increasing layer thickness (when the thicknesses are below roughly 1 micron) and also with the general improvement of the material quality over the years.
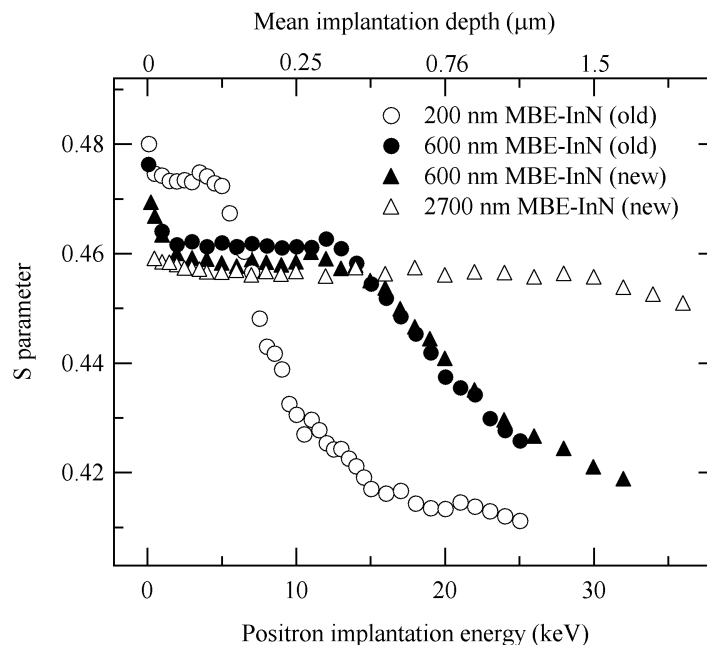
Figure 2. The S parameter measured as a function of positron implantation energy in selected MBE-grown InN layers.

The thickest (2700 nm) InN layer is essentially defect-free from the point of view of positrons [29]. The increased S parameter in the other layers indicates that the positron-electron momentum distribution is narrower than in the defect-free reference sample. The narrowing is due to positrons annihilating as trapped at vacancy defects, where the electron density is lower and the probability of annihilation with high-momentum core electrons is reduced compared to that of delocalized positrons in the lattice. Hence the increased S parameter is a clear sign of vacancy defects present in the measured layers. When the S and W parameters of the InN layers are plotted as function of each other

(not shown, see Ref. [28]) they form a line indicating that positrons annihilate from two different states. These have been identified as the delocalized state in the InN lattice and the In vacancy by combining Doppler broadening and positron lifetime measurements [28], the latter performed with a pulsed positron beam.

The concentration of V_{In} can be estimated from the S parameter data with the positron trapping model. When the cation vacancies are the only defects trapping positrons, their concentration can be determined with the simple formula

$$[V_{In}] = \frac{N_{at}(S - S_B)}{\mu_V \tau_B (S_V - S)},$$ (5)

where τ_B = 185 ps is the positron lifetime in the InN lattice [28], $\mu_V = 3 \times 10^{15}$ s^{-1} is the positron trapping coefficient [1, 28] and $N_{at} = 6.367 \times 10^{22}$ cm^{-3} is the atomic density of InN. For the S parameter at the In vacancies we take S_V/S_B = 1.050 [28, 29]. From these values, the In vacancy concentrations can be extracted to be in the $10^{16} - 10^{19}$ cm^{-3} range in the different layers. The In vacancy concentration has been shown to decrease dramatically with the layer thickness in the first micron, and to correlate negatively with the electron mobility suggesting that the In vacancies act as important scattering centers in InN, although their concentration is typically not sufficient for efficient compensation of the *n*-type conductivity [28]. Interestingly, the formation of In vacancies seems not to be influenced by the growth stoichiometry in MOCVD growth [30], and recent results suggest this holds also in the case of MBE growth [31].

As in the case of GaN, irradiation experiments have been performed in InN in order to study the introduction of In vacancies and their recovery in subsequent thermal treatments [29]. It has been shown that light particle irradiation produces In vacancies, but with an introduction rate more than one order of magnitude lower than that of Ga vacancies in GaN. Instead, intrinsic negative ion type defects are produced at a similar rate as in GaN, indicating that they are the dominant compensating defects in irradiated n-type InN. In fact, InN becomes more n-type in the irradiation experiments, and it has been suggested that this is due to the production of N vacancies that would act as donors [32]. The results obtained with positrons both before and after [31] the thermal treatments support the existence of a high concentration of N vacancies in the irradiated material, even if the N vacancies have not been observed directly.

4.2. Vacancy defects in AlN

Figure 3 presents the average positron lifetime measured as a function of temperature in bulk AlN crystal [33] grown by physical vapor transport (PVT) [34] together with the data from a bulk HNP-GaN sample [10]. The temperature dependence of the average lifetime τ_{ave} measured in AlN is qualitatively similar to that of GaN. It is constant, about 158 ps, at temperatures below 300 K, above which it starts increasing with increasing temperature reaching about 170 ps at 600 K. The lifetime spectra recorded at 450 – 600 K can be decomposed into two components, the longer of which (not shown in the figure) is constant, τ_2 = 210 ± 15 ps, as a function of temperature. By comparison to GaN, the behavior as a function of temperature is interpreted as the competition of negative ion type defects (shallow traps with no open volume) and vacancy defects in trapping of positrons. The longer lifetime component has been preliminarily attributed to Al vacancies [33], and the positron lifetime of the AlN lattice has been estimated to be about 155 ps.

The concentrations of both the Al vacancies and the negative ions can be estimated from the data using Eqs. (1) – (4) and assuming a trapping coefficient of $\mu_V = 3 \times 10^{15}$ cm^{3}s^{-1} for the Al vacancies at 300 K. The Al vacancy concentration of about 1×10^{17} cm^{-3} is extracted from the data measured at 600 K, taking into account the temperature dependence of the trapping coefficient, and gives a lower limit estimate as the lifetime still increases at this temperature as seen in figure 3. However, as the increase of τ_{ave} with temperature seems to slow down when approaching 600 K, the actual vacancy

concentrations are not likely to be more than twice the estimated values. The concentration of the negative ions can be estimated from the data below 300 K, where no thermal escape from the hydrogenic states is observed, giving $c_{st} \approx 4 \times 10^{18}$ cm^{-3}. It is important to note that the concentration of the negative ions is an order of magnitude higher than that of the Al vacancies, hence making them the dominant negative (acceptor) centers in AlN, while in GaN with a similar O content the concentrations of Ga vacancies and negative ions are similar. Surprisingly, the comparison of the concentrations of impurities and negative ions suggests that the latter could be related to oxygen rather than to carbon impurities. It should be noted, though, that in contrast to the situation in GaN, O in AlN has been predicted to exhibit negative charge states as well [33].
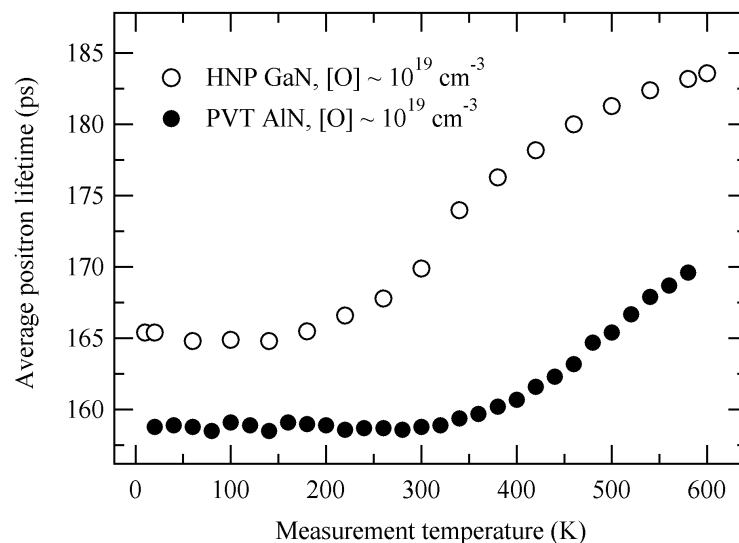
Figure 3. The average positron lifetime measured as a function of temperature in bulk GaN and AlN samples.

In addition to bulk crystal growth, both MBE and MOCVD have been used to grow AlN thin films on different substrates. Some positron studies have been performed on both kinds of materials [35, 36]. However, as proper identification of the vacancy and lattice parameters combining Doppler broadening and positron lifetime experiments is still lacking, the interpretations need to be considered with reasonable care. The results are comparable to those obtained in other nitrides (and semiconductors in general) in the sense that higher lattice mismatch between the substrate and the AlN layer seems to lead to a higher S parameter (and hence to a higher vacancy content). In addition, the dependence of the vacancy content on the growth stoichiometry seems to be rather weak for low V/III ratios, but effects become visible at very high V/III ratios. Finally, as in the case of GaN and InN, a higher growth temperature causes a higher vacancy content.

5. Discussion
As the positron research in InN and AlN is still rather scarce, it is difficult to make a full comparison of the three nitride materials. However, many properties can be compared separately between InN and GaN, and AlN and GaN. In the case of bulk GaN and AlN crystals, it is fascinating to observe that similar kind of interplay of vacancies and negative ion type defects (most likely impurities) is found, in spite of the difference between the conductivities: GaN is quite heavily *n*-type, while the Fermi level in AlN is more than 1 eV below the conduction band minimum making it "almost" *n*-type. However, even if in GaN the in-grown vacancies are bound to O impurities, in AlN this might not be the case due to the possible negative charge of the O impurities at sufficiently high Fermi level positions. It should be noted that the formation energy of a V_{Al}–O_N pair is predicted to be lower than that of a single Al vacancy [19], but the lack of suitable direct formation sites for the pair makes it

probable that these pairs would form in AlN in a similar manner as in GaN, i.e., by formation of isolated vacancies and pairing during cooling down. However, if both the constituents of the complex are negatively charged when isolated, it is likely that there is quite a high barrier to be overcome during migration and pair formation.

Irradiation experiments have been performed in InN and GaN, but for the time being not in AlN. These experiments have shown that GaN behaves "normally" in the particle irradiation experiments, i.e., the introduction rates of the defects on both sublattices are on an expected level, both based on theory and other semiconductor materials [12]. Naturally there are unresolved issues, such as why some of the irradiation-induced Ga vacancies survive very high annealing temperatures (up to 800ºC), and what are the exact effects of hydrogen as it is the only impurity abundant enough in high-quality undoped material to create complexes with a significant fraction of vacancies. In InN on the other hand, the production of In vacancies in particle irradiation is much slower than that could be expected, and in light of other peculiarities of the material (among others, the Fermi level in InN moves away from the midgap instead of approaching it in the irradiation) it has been proposed that the In vacancies undergo a similar acceptor-to-donor transition as the $V_{Ga} \leftrightarrow V_{As}+As_{Ga}$ transition in GaAs [29]. In fact, the recent annealing experiments suggest that very efficient vacancy clustering takes place already at very low In vacancy concentrations, supporting the view that very high N vacancy concentrations are present after the irradiation, and that some of them might actually originate from the above-mentioned complexes.
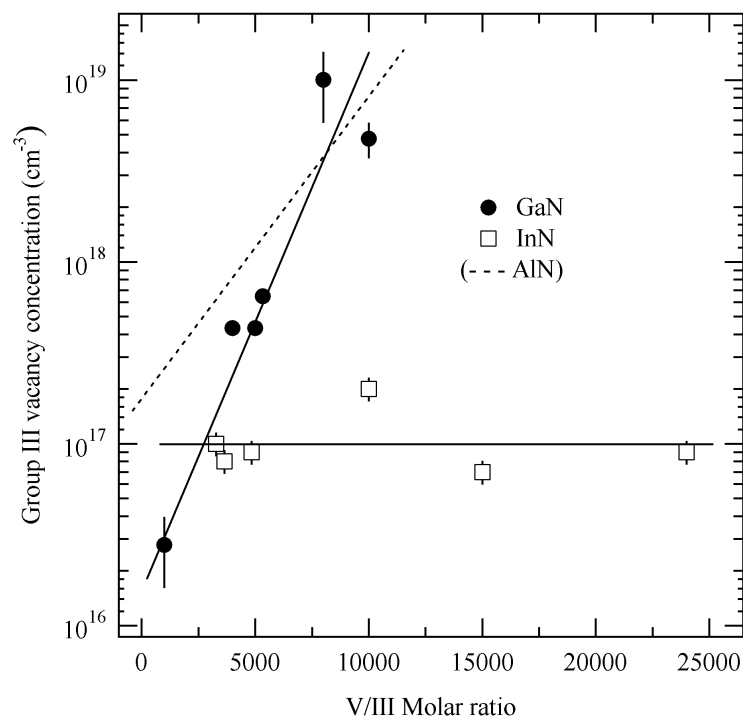
Figure 4. The cation vacancy concentrations in MOCVD-grown III-nitrides as a function of the growth stoichiometry. The results for AlN should be considered preliminary.

The three nitride materials can be compared in terms of vacancy formation in different MOCVD growth conditions. In all three materials, a higher growth temperature results in a higher vacancy concentration. On the other hand, other growth parameters can have different effects. Figure 4 shows the concentrations of Ga, In and Al vacancies in GaN, InN and AlN, respectively, as a function of the V/III ratio during growth. The difference in the behavior of the cation vacancies in GaN, InN and AlN

is evident: the growth stoichiometry has no effect on the vacancy content in InN, while the effects are clear in GaN and AlN – the higher the V/III ratio the higher the III-vacancy concentration. A plausible explanation for the differences can be found in the vacancy formation energies and the temperatures of the MOCVD growth. In *n*-type (or "almost" *n*-type for AlN) material, the calculated formation energy of the Ga and Al vacancies is about 1 eV, while it is almost 3 eV for the In vacancy [19,37]. On the other hand, the growth temperature of AlN and GaN is around or above 1000 ºC, but only around 500–600ºC in the case of InN. As the concentrations of the Ga, Al and In vacancies are similar in the samples with low V/III ratios, the formation of the In vacancies must be dictated by other effects, such as strain or presence of dislocations, than the thermal formation (and subsequent stabilization by e.g. impurities) of an isolated In vacancy in an otherwise perfect lattice. On the other hand, the observed Al and Ga vacancy concentrations are of the same order of magnitude as could be expected from the growth temperature and the calculated formation energy, given that the vacancies (which are mobile already at relatively low temperatures) are stabilized by impurities (such as O in GaN) or other defects relatively close to the growth temperature. Hence it can be understood why the stoichiometric conditions affect the final Ga vacancy concentration in GaN and possible Al concentration in AlN more than the In vacancy concentration in InN.

The future directions in nitride research with positrons are varied. Concerning the fundamental material properties, the basic understanding of the vacancy defects and their interactions with impurities and other defects in all three materials needs to improved, especially in InN and AlN that have been studied much less than GaN. To this end systematic studies of effects of both *n*- and *p*-type doping (when possible) and of growth conditions, including polarity, need to be performed in addition to irradiation experiments also at low temperatures that provide valuable information on isolated intrinsic defects. A subject not touched upon in this paper is ion implantation and the defects induced by this kind of processing, although some studies already exist [38, 39]. As this is a standard processing technique in semiconductor technology, and is becoming an attractive way of making devices in nitrides as well, the produced defects and their impact should be better understood.

Up to now mostly binary alloys have been studied, with just a handful of papers published on ternary alloys such as $In_{1-x}Ga_xN$ or $Al_{1-x}Ga_xN$ [40, 41]. However, these are the materials that are of very high technological interest as they form the active layers in opto-electronic devices. The preliminary experiments that have been performed suggest that the vacancies in these ternary and eventually quaternary alloys do not behave in a similar manner as in the binary constituents. Hence these materials should and probably will be studied in the near future. Finally, closely related to the ternary alloys, quantum structures and possibly quantum dots will be the subject of future studies. The nitride quantum structures provide an interesting playground for both theoretical and experimental positron physics thanks to the polarization-induced in-grown saw-tooth-like electric fields in the wurtzite heterostructures [42–44]. Positrons are prone to be localized by the electric fields at the interfaces of such structures, and hence they could provide information about the local atomic configurations of the interfaces that may have a significant impact on device operation.

6. Summary

A short review and comparison of the results obtained with positron annihilation spectroscopy in studies of vacancy defects in AlN, GaN and InN are presented. The efficient use of positron lifetime and Doppler broadening techniques complemented by theoretical calculations has given the possibility to deduce both the identities and the concentrations of the vacancies in these materials. Measurements as a function of temperature have given information on the charge states of the detected defects. The III-sublattice vacancies are common defects in all the III-nitrides, and they compensate donors either by forming vacancy-impurity complexes or by providing deep states for electrons. In some cases also N vacancies have been observed. The formation of these defects under different growth conditions has been studied in the three materials. Also the effects of particle irradiation have been explored.

References

[1]   Saarinen K, Laine T, Kuisma S, Nissilä J, Hautojärvi P, Dobrzynski L, Baranowski J M, Pakula K, Stepniewski R, Wojdak M, Wysmolek A, Suski T, Leszczynski M, Grzegory I and Porowski S 1997 *Phys. Rev. Lett.* **79** 3030

[2]   Saarinen K, Hautojärvi P and Corbel C 1998 *Identification of Defects in Semiconductors* (*Semiconductors and Semimetals* vol 51A) ed Stavola M (New York: Academic Press) p 209

[3]   Tuomisto F, Suski T, Teisseyre H, Krysko M, Leszczynski M, Lucznik B, Grzegory I, Porowski S, Wasik D, Witowski A, Gebicki W, Hageman P and Saarinen K 2003 *Phys. Status Solidi (b)* **240** 289

[4]   Saarinen K, Seitsonen A P, Hautojärvi P and Corbel C 1995 *Phys. Rev. B* **52** 10932

[5]   Corbel C, Pierre F, Saarinen K, Hautojärvi P and Moser P 1992 *Phys. Rev. B* **45** 3386

[6]   Puska M J, Corbel C and Nieminen R M 1990 *Phys. Rev. B* **41** 9980

[7]   Alatalo M, Kauppinen H, Saarinen K, Puska M J, Mäkinen J, Hautojärvi P and Nieminen R M: 1995 *Phys. Rev. B* **51** 4176

[8]   Asoka-Kumar P, Alatalo M, Ghosh V J, Kruseman A C, Nielsen B and Lynn K G 1996 *Phys. Rev. Lett.* **77** 2097

[9]   According to Web of Science® by Thomson Scientific in July 2008

[10]   Tuomisto F, Saarinen K, Lucznik B, Grzegory I, Teisseyre H, Suski T, Porowski S, Hageman P R and Likonen J 2005 *Appl. Phys. Lett.* **86** 031915

[11]   Hautakangas S, Ranki V, Makkonen I, Puska M J, Saarinen K, Xu X and Look D C 2006 *Phys. Rev. B* **73** 193301

[12]   Tuomisto F, Ranki V, Look D C and Farlow G C 2007 *Phys. Rev. B* **72** 165207

[13]   Oila J, Kivioja J, Ranki V, Saarinen K, Look D C, Molnar R J, Park S S, Lee S K and Han J Y 2003 *Appl. Phys. Lett.* **82** 3433

[14]   Saarinen K, Hautakangas S and Tuomisto F 2006 *Phys. Scripta* **T126** 105

[15]   Tuomisto F, Hautakangas S, Makkonen I, Ranki V, Puska M J, Saarinen K, Bockowski M, Suski T, Paskova T and Monemar B 2006 *Phys. Status Solidi (b)* **243** 1436

[16]   Saarinen K, Suski T, Grzegory I and Look D C 2001 *Phys. Rev. B* **64** 233201

[17]   Paskova T, Hommel D, Paskov P P, Darakchieva V, Monemar B, Bockowski M, Suski T, Grzegory I, Tuomisto F, Saarinen K, Ashkenov N and Schubert M 2006 *Appl. Phys. Lett.* **88** 141909

[18]   Tuomisto F, Saarinen K, Bockowski M, Suski T, Paskova T and Monemar B 2006 *J. Appl. Phys.* **99** 066105

[19]   Mattila T and Nieminen R M 1997 *Phys. Rev. B* **55** 9571

[20]   Neugebauer J and Van de Walle C G 1996 *Appl. Phys. Lett.* **69** 503

[21]   Tuomisto F, Paskova T, Figge S, Hommel D and Monemar B 2007 *J. Crystal Growth* **300** 251

[22]   Tuomisto F, Paskova T, Kröger R, Figge S, Hommel D, Monemar B and Kersting R 2007 *Appl. Phys. Lett.* **90** 121915

[23]   Oila J, Ranki V, Kivioja J, Saarinen K, Hautojärvi P, Likonen J, Baranowski J M, Pakula K, Suski T, Leszczynski M and Grzegory I 2001 *Phys. Rev. B* **63** 045205

[24]   Hautakangas S, Oila J, Alatalo M, Saarinen K, Liszkay L, Seghier D and Gislason H P 2003 *Phys. Rev. Lett.* **90** 137402

[25]   Hautakangas S, Saarinen K, Liszkay L, Freitas, Jr. J A and Henry R L 2005 *Phys. Rev. B* **72** 165303

[26]   Rummukainen M, Oila J, Laakso A, Saarinen K, Ptak A J and Myers T H 2004 *Appl. Phys. Lett.* **84** 4887

[27] Saarinen K, Seppälä P, Oila J, Hautojärvi P, Corbel C, Briot O and Aulombard R L 1998 *Appl. Phys. Lett.* **73** 3253

[28] Oila J, Kemppinen A, Laakso A, Saarinen K, Egger W, Liszkay L, Sperr P, Lu H and Schaff W J 2004 *Appl. Phys. Lett.* **84** 1486

[29] Tuomisto F, Pelli A, Yu K M, Walukiewicz W and Schaff W 2007 *Phys. Rev. B* **75** 193201

[30] Pelli A, Saarinen K, Tuomisto F, Ruffenach S and Briot O 2006 *Appl. Phys. Lett.* **89** 011911

[31] Reurings F, Rauch C, Tuomisto F, Jones R E, Yu K M, Walukiewicz W and Schaff W J 2010 *Phys. Rev. B* **82** 153202; Reurings F, Tuomisto F, Gallinat C S, Koblmüller G and Speck J S, *Appl. Phys. Lett.*, in press

[32] Li S X, Yu K M, Wu J, Jones R E, Walukiewicz W, Ager III J W, Shan W, Haller E E, Lu H and Schaff W J 2005 *Phys. Rev. B* **71** 161201

[33] Tuomisto F, Mäki J-M, Chemekova T Yu, Makarov Yu N, Avdeev O V, Mokhov E N, Segal A S, Ramm M G, Davis S, Huminic G, Helava H, Bickermann M and Epelbaum B M 2008 *J. Crystal Growth* **310** 3998

[34] Bickermann M, Epelbaum B M and Winnacker A 2004 *J. Crystal Growth* **269** 432

[35] Koyama T, Sugawara M, Hoshi T, Uedono A, Kaeding J F, Sharma R, Nakamura S and Chichibu S F 2007 *Appl. Phys. Lett.* **90** 241914

[36] Mäki J-M, Tuomisto F, Bastek B, Bertram F, Christen J, Dadgar A and Krost A 2009 *Phys. Status Solidi (c)* **6** 2575

[37] Stampfl C, Van de Walle C G, Vogel D, Krüger P and Pollmann J 2000 *Phys. Rev. B* **61** R7846

[38] Nakano Y and Kachi T 2002 *J. Appl. Phys.* **91** 884

[39] Uedono A, Ito K), Nakamori H, Mori K, Nakano Y, Kachi T, Ishibashi S, Ohdaira T, Suzuki R 2007 *J. Appl. Phys* **102** 084505

[40] Onuma T, Chichibu S F, Uedono A, Sota T, Cantu P, Katona T M, Keading J F, Keller S, Mishra U K, Nakamura S and DenBaars S P 2004 *J. Appl. Phys.* **95** 2495

[41] Slotte J, Tuomisto F, Saarinen K, Moe C G, Keller S and DenBaars S P 2007 *Appl. Phys. Lett.* **90** 151908

[42] Bernardini F, Fiorentini V and Vanderbilt D 1997 *Phys. Rev. B* **56** 10024

[43] Fiorentini V, Bernardini F, Della Sala F, Di Carlo A and Lugli P 1999 *Phys. Rev. B* **60** 8849

[44] Lefebvre P, Morel A, Gallart M, Taliercio T, Allegre J, Gil B, Mathieu H, Damilano B, Grandjean N and Massies J 2001 *Appl. Phys. Lett.* **78** 1252